Experimental Study Regarding PA and PE Sheets on Single Point Incremental Forming Process

Nicolae Rosca[1], *Mihaela* Oleksik [1,*], and *Valentin* Oleksik [2]

[1]Lucian Blaga University of Sibiu, Department of Industrial Engineering and Management, 10 Victoriei Bd, Sibiu, Romania

[2]Lucian Blaga University of Sibiu, Department of Machines and Industrial Equipment's, 10 Victoriei Bd, Sibiu, Romania

Abstract. The present paper aims to present an experimental study on the behaviour of PA and PE sheets during the single point incremental forming. Due to the fact that the purpose of this research is to study the behaviour of PA and PE sheets during the single point incremental process both in terms of process forces and in terms of major and minor strain and thickness reduction, a Kuka Kr210 robot was chosen as an alternative to using a universal milling machine. The specimens were made of 3 mm PA and PE sheets. The size of the sheets was 250 mm x 250 mm. The forces measured on the three directions of the coordinate axes were compared. To measure the major strain, minor strain and thickness reduction, the digital image correlation method was applied.

1 State of the art

The single point incremental forming process is a metal forming process that has been gaining recognition in recent years due to its main advantage, namely the reduction of manufacturing costs because of the simplicity of the forming tools it uses [1].

One of the first papers that analyse the thermoplastic materials at SPIF is the paper of Martins et al. [2], which determines the process limits. They found many similarities between the morphology of the polymer cracks and those that are usually found in the SPIF of metals. They also established that a high formability can be obtained in the SPIF of polymers.

A numerical simulation analysis was conducted to identify the formability of polycarbonate sheets for several part geometries, obtained with different wall angles [3]. The geometries used were frustum of pyramid, frustum of triangular prisms and frustum of cone, and the authors pointed out that it is possible to obtain parts with tilt angles of up to 82^0, much larger than those in the case of metallic materials. The plastic flow and failure mechanism during the SPIF were also analysed for PVC sheets [4]. The forming mechanism during SPIF of polycarbonate sheets and high-density polyethylene was studied considering a strategy of reducing bulging effects [5]. The authors found that the accuracy of the parts obtained by SPIF in the case of polymeric materials is lower than that of metallic materials

* Corresponding author: mihaela.oleksik@ulbsibiu.ro

and developed a strategy to increase the geometric accuracy. Another direction of research consisted of measuring the springback in polypropylene sheets manufactured by SPIF [6].

The forces during the SPIF of different polymeric materials were analysed by Medina-Sanchez et al. [7]. This study was a combined analytical-numerical-experimental study for polycarbonate sheets and polyvinylchloride sheets. The authors validated the analytical and numerical studies, as they obtained a less than 10% error range compared to the experimental research. Another study considered both the forces in the single point incremental forming process, as well as the effects of temperature on polyvinylchloride sheets [8]. Another paper analysed the single point incremental forming of polymer sheets based on the electric energy consumption and cost criteria [9]. The process parameters were evaluated to reduce the energy consumption with a direct influence on environmental pollution.

Another study referred to the ability of polymeric materials of self-heating during the SPIF process [10]. They studied the SPIF behaviour of PC sheets by modifying the punch rotation speed and the traveling speed and measuring their influence on the process temperature. They found that with the increase of the punch rotation speed and the decrease of the traveling speed, the formability of polycarbonate sheets improved due to the self-heating process.

The effects of the vertical step and punch rotation speed on the failure modes and microstructural properties during the SPIF were studied by Davarpanah et al. [11]. The authors showed that a larger vertical step led to increased void densities, as well as the fact that the structure of the polymer sheet becomes more crystalline following the deformation. Two materials were studied: petroleum-based PVC sheet and bio-based polylactic acid (PLA) sheet with different thicknesses.

Other very recent papers used FEM to analyse the behaviour of polymer sheets during SPIF [12, 13]. The numerical simulations used a thermomechanical coupled model, in order that the simulation also took into consideration the self-heating phenomenon that occurs in these materials. The numerical simulations were validated by experimental research.

The main possibilities of implementing manufacturing by SPIF were presented by Marques et al. [14], while Bagudanch et al. [15] presented a possible application of single point incremental forming of polymer sheets in the manufacturing of cranial implants made of biocompatible polymer.

Not only simple polymeric materials can be manufactured by single point incremental forming, but also composite polymeric materials [16], shape memory polymer foam [17] or multilayer materials made of two different thermoplastics [18].

Having analysed the results of previous research, this paper aims to analyse a comparative experimental study on two polymeric materials: polyamide (PA) and polyethylene (PE) from the perspective of the major strain, minor strain and thickness reduction, as well as of the process forces.

2 Materials and method

The uniaxial tensile test of PA and PE materials was conducted using the Instron 5587 universal traction, compression and buckling testing machine, with a maximum load capacity of 300 kN, a maximum specimen elongation of 800 mm and an adjustable test speed in the range of 0.001 - 500 mm/min. The test machine is equipped with a load cell of +/- 0.25% linearity and +/- 0.25% repeatability of outputs ranging between 0.4 and 100% of the capacity. Two sets of 3 specimens for each type of polymer sheet were made using the water cutting process. The standardized form of the polymer material was chosen for the tensile test, the testing speed was set at 7 mm/s (a speed equal to the speed imposed to the robot in case of experiments related to single point incremental forming), and the acquisition rate of the test machine was of 10 points per second.

Figure 1 presents the experimental layout used in the manufacturing by single point incremental forming of PA and PE sheets, with the Aramis optical analyser (figure 1, a) and force transducer. The trajectory used was a trajectory equivalent to a cone-frustum with a lower base of 85 mm, the height of the part was 40 mm, the punch used had a 8 mm diameter, and the vertical step was 0.75 mm (figure 1, b). We chose a spiral trajectory in order to define the cone-frustum trajectory to avoid the local penetrations of the punch. The Kuka Kr210 robot, which has a maximum force of 2000 N, was used to perform the experiments related to the single point incremental forming. The advantage of using a robot for this metal forming process consists in the fact that the vertical positioning of the blank sheet allows the on-line measurement of the main strains and thickness reduction. The major disadvantage of using industrial robots in forming processes, namely the low rigidity and implicitly the reduced dimensional accuracy, does not affect us in this case, because the loads to which the robot is subjected are much lower than in the case of single point incremental forming of metals.

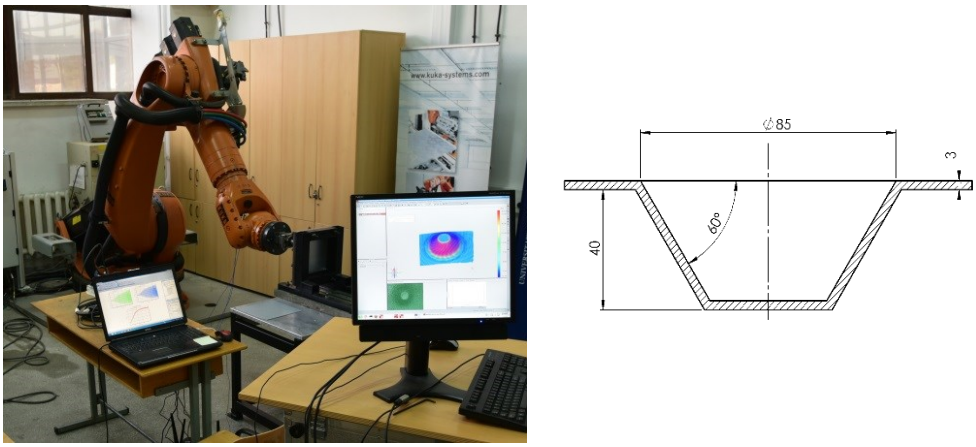

(a) (b)

Fig. 1. The forming equipment for SPIF of polymer sheet (a); Part geometry (b)

The Aramis real-time optical measurement system was used for the local determination of the main strains. To perform a deformation determination experiment, it is necessary to calibrate the measurement system. A series of gauges of different dimensions were used for this purpose, dimensions which are found in the equipment of the measuring system, depending on the size of the area to be measured. A calibre measuring 120 x 120 mm was used in the present research. The aperture of the optical camera and the exposure time were then adjusted, between which there must be a good correlation so that there are no underexposed, nor overexposed areas. The calibration consists in the acquisition of several 12-18 successive images in which the measurement system can identify certain markers that are found on the calibres. By identifying these markers, the 3D space in which the operating system can operate with the lowest possible error rate was delimited. To be able to carry out experimental research with the help of the Aramis measurement system, it was necessary to previously apply a network of points on the surface of the part. Having the specimens thus prepared, the testing process was started, with the acquisition of 1 image/second, to have the best possible continuity of the measurement process. For the determination of the the principal strains the thinning, the shear angle, as well as the Von Misses equivalent strain and the Tresca strain additional calculations were performed.

The PCB 261A13 force sensor which allows, along with the Quantum X MX840B digital acquisition system and the CMD 600 digital charge amplifier, was use for force measuring during the single point incremental forming process.

Although the force sensor allows the measurement of forces up to 44 kN on the direction perpendicular to the blank sheet plane (z direction) and 19 kN on the directions in the blank sheet plane (x and y direction), due to the fact that the forces required for the single point incremental forming of polymers are of much lower values, the sensor was calibrated using the Instron 5587 testing machine in the range of 0 … 1 kN for the direction perpendicular to the blank sheet plane (z direction), and 0 … 500 N for the directions in the blank sheet plane (x and y direction), respectively. The force sensor is mounted on the arm of the Kuka Kr210 robot, having the punch clamping system attached to it.

Three sets were made of both PA and PE blank sheets with a size of 250 x 250 mm and a thickness of 3 mm.

3 Results

The results of the tensile tests for PA and PE, together with the statistical processing of the results are presented in table 1 and table 2.

Table 1. Results for uniaxial tensile test for PA specimens

Specimen number / Statistic data	E Modulus [MPa]	Yield Stress [MPa]	Maximum Tensile Stress [MPa]	Maximum elongation [%]
1	524.86	15.19	41.11	161.88
2	518.03	17.43	40.82	135.30
3	488.69	16.98	40.01	129.86
Mean	510.53	16.53	40.65	142.35
Median	518.03	16.98	40.82	135.30
St. deviation	19.22	1.185	0.570	17.13
p-value	0.232	0.251	0.358	0.205

Table 2. Results for uniaxial tensile test for PE specimens

Specimen number / Statistic data	E Modulus [MPa]	Yield Stress [MPa]	Maximum Tensile Stress [MPa]	Maximum elongation [%]
1	145.05	13.78	24.74	504.61
2	148.36	13.69	24.81	482.30
3	132.02	13.56	24.68	488.02
Mean	141.81	13.68	24.74	491.64
Median	145.05	13.69	24.74	488.02
St. deviation	8.64	0.111	0.065	11.59
p-value	0.253	0.576	0.620	0.345

The graphs in engineering strain - engineering stress curves are shown in Figure 2, a and b. The longitudinal elastic modulus, yield stress, maximum tensile stress and maximum elongation were measured. From a statistical point of view, the mean, median, standard deviation and p-value are presented for the Anderson-Darling test. As can be seen in all cases, the p-value is greater than 0.05 for all measured values, thus the null hypothesis is respected.

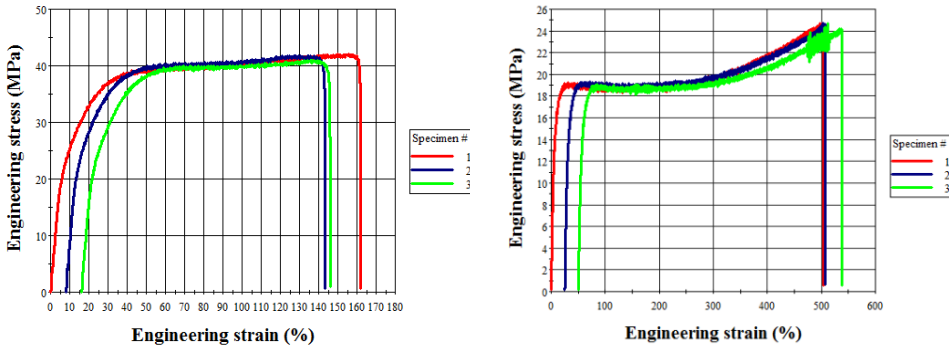

Fig. 2. Stress-strain curve for PA sheet (a); Stress-strain curve for PE sheet (b)

The average value of the E modulus is 510.53 MPa for PA and 141.81 for PE, respectively. The analysis of these values shows that the average value of the E modulus in the case of PA is about 3.6 times higher than in the case of PE. The average value of the Yield stress is 16.53 MPa for PA and 13.68 for PE, respectively. As far as the maximum tensile stress is concerned, the average value for PA is 40.65 MPa compared to 24.74 MPa for PE. Regarding the maximum elongation, things are reversed, as the average values are 491.64% and 142.35% for PE and PA, respectively. These values highlight the fact that the PE sheets have a maximum elongation 3.45 times higher than that of the PA sheets.

Tables 3 and 4 show the quantitative results for the strain on the x direction, the strain on the y direction, the major strain, minor strain, thickness reduction and shear angle for the PA and PE sheets manufactured by SPIF. In this case also, data was analysed from a statistical point of view, again by means of the Anderson-Darling test, leading to the observation that the experimental data is normally distributed, with no aberrant values.

Table 3. The main deformation's results for PA specimens

Specimen number / Statistic data	Strain on x-direction [mm/mm]	Strain on y-direction [mm/mm]	Major strain [mm/mm]	Minor strain [mm/mm]	Thickness reduction [mm/mm]	Shear angle [degrees]
1	0.750	0.766	0.772	0.097	0.854	35.81
2	0.742	0.756	0.761	0.105	0.841	35.86
3	0.781	0.771	0.790	0.091	0.851	35.42
Mean	0.758	0.764	0.774	0.098	0.848	35.70
Median	0.750	0.756	0.772	0.097	0.851	35.81
St. deviation	0.021	0.008	0.015	0.007	0.007	0.241
p-value	0.257	0.487	0.541	0.596	0.300	0.136

Figures 3, 5, 7, 9 and 11 show different strains for PA sheets, while figures 4, 6, 8, 10 and 12 show the same strains for PE sheets. The logarithmic strain is presented for all images.

The analysis of the images finds a distribution of deformations located in the direction taken into consideration for the strains on the x-direction and y-direction, respectively, which is absolutely normal, a relatively uniform distribution of the major strain and thickness reduction on the wall part area, and a localization of maxima of the minor strain towards the highest area of the part, more pronounced in the case of PA sheets. As far as the shear angle is concerned, it varies from positive to negative values, keeping the same extreme values for each material.

Table 4. The main deformation's results for PE specimens

Specimen number / Statistic data	Strain on x-direction [mm/mm]	Strain on y-direction [mm/mm]	Major strain [mm/mm]	Minor strain [mm/mm]	Thickness reduction [mm/mm]	Shear angle [degrees]
1	0.592	0.597	0.599	0.097	0.681	29.18
2	0.623	0.610	0.611	0.091	0.694	29.45
3	0.581	0.579	0.603	0.092	0.678	29.32
Mean	0.599	0.595	0.604	0.093	0.684	29.32
Median	0.581	0.597	0.603	0.092	0.681	29.32
St. deviation	0.022	0.015	0.006	0.003	0.008	0.135
p-value	0.355	0.586	0.487	0.200	0.230	0.628

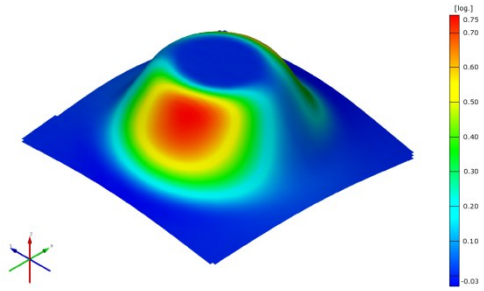

Fig. 3. Strain on x direction for PA sheet

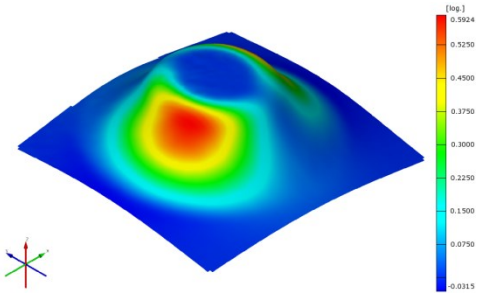

Fig. 4. Strain on x direction for PE sheet

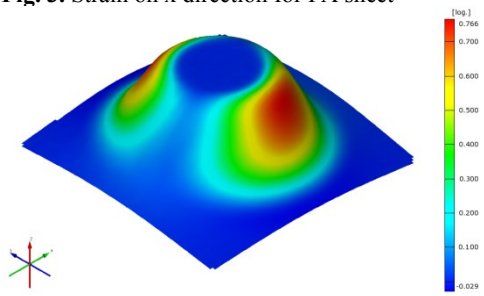

Fig. 5. Strain on y direction for PA sheet

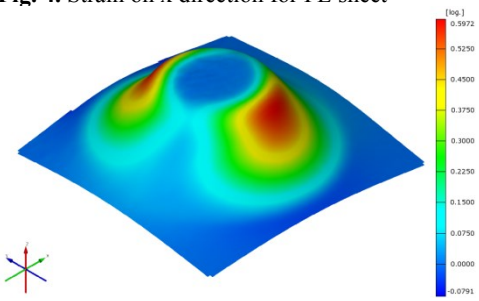

Fig. 6. Strain on y direction for PE sheet

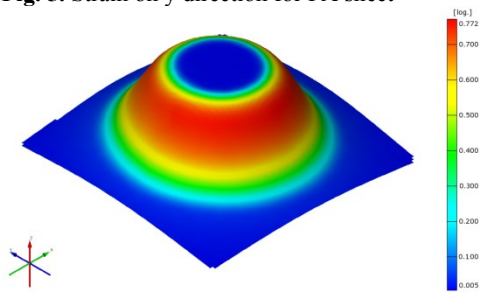

Fig. 7. Major strain for PA sheet

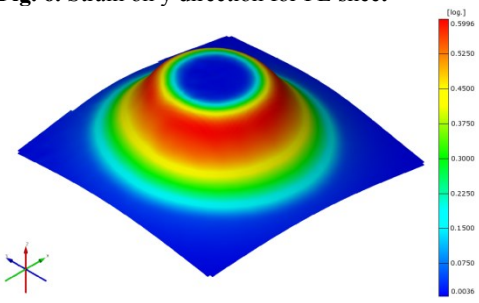

Fig. 8. Major strain for PE sheet

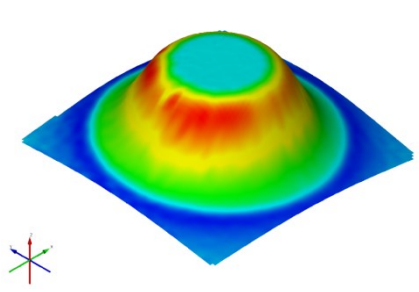

Fig. 9. Minor strain for PA sheet

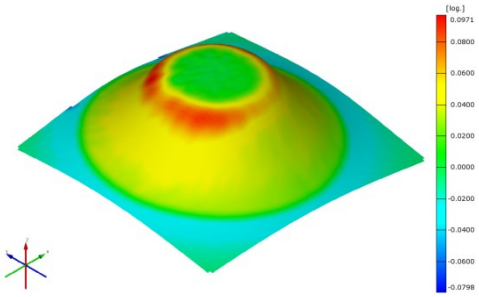

Fig. 10. Minor strain for PE sheet

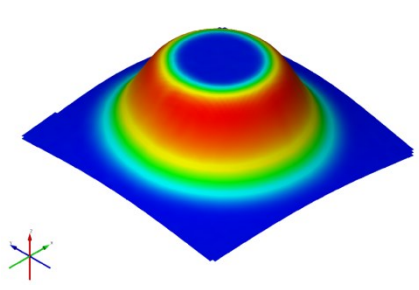

Fig. 11. Thickness reduction for PA sheet

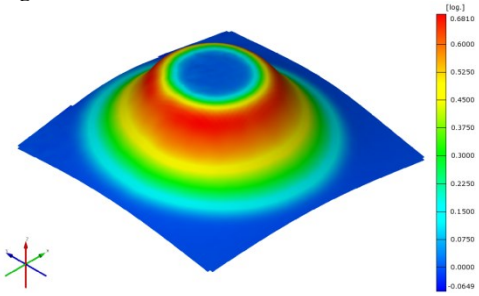

Fig. 12. Thickness reduction for PE sheet

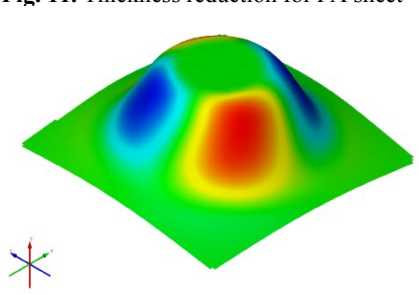

Fig. 13. Shear angle for PA sheet

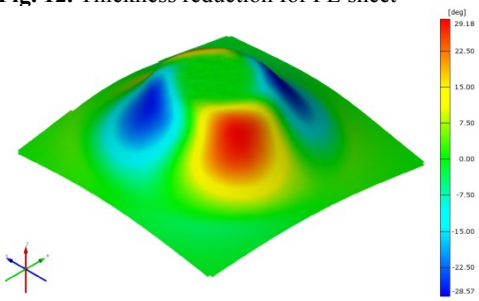

Fig. 14. Shear angle for PE sheet

A first observation consists in the fact that both materials have a strong elastic springback, which is mostly visible in the case of PE sheets. It should be emphasized once again that both types of materials were manufactured using the same punch trajectory. Of course, in both the cases of PA and PE sheets, the average values of the strain on the x direction and the strain on the y direction are similar due to the conical shape of the trajectory. When comparing these values between the two materials, an average value of 0.758 mm/mm is observed for the strain on the x direction and of 0.764 mm/mm for the strain on the y direction for PA sheets, while in the case of PE sheets, the average values are of 0.599 mm/mm for the strain on the x direction and of 0.595 mm/mm for the strain on the y direction, respectively. In the case of the major strain, the average value is 0.774 mm/mm for the PA sheets and 0.604 mm/mm for the PE sheets. Regarding the minor strain, the average values are very close: 0.097 mm/mm and 0.093 mm/mm for PA and PE sheets, respectively. The average values of the shear angle are 35.700 in the case of PA sheets and 29.320 in the case of PE sheets. The lower values in most cases of the PE sheets are, as previously stated, due to their stronger spring back compared to the PA sheets. This phenomenon is related, as was natural, to the value of the E modulus, being known that a low value of the E modulus leads to an increase in the spring back.

Tables 5 and 6 show the quantitative results for the force on the x-direction, the force on the y-direction and the force on the z-direction for PA and PE sheets manufactured by SPIF.

In order to verify the distribution of the experimental data, the p-values for the Anderson-Darling test are again observed to be greater than 0.05, thus following a normal repartition.

Table 5. The force's results for PA specimens

Specimen number / Statistic data	Force on x-direction [kN]	Force on y-direction [kN]	Force on z-direction [kN]
1	0.322	0.326	0.802
2	0.328	0.329	0.810
3	0.331	0.330	0.789
Mean	0.327	0.328	0.800
Median	0.328	0.326	0.802
St. deviation	0.005	0.002	0.011
p-value	0.487	0.334	0.543

Table 6. The force's results for PE specimens

Specimen number / Statistic data	Force on x-direction [kN]	Force on y-direction [kN]	Force on z-direction [kN]
1	0.274	0.280	0.535
2	0.276	0.277	0.521
3	0.281	0.282	0.539
Mean	0.277	0.280	0.532
Median	0.276	0.280	0.535
St. deviation	0.004	0.003	0.009
p-value	0.399	0.565	0.285

Figures 15, 17 and 19 and 16, 18 and 20, respectively, show the variation of the forces in the single point incremental forming process on the three directions of the coordinate axes. Regarding the maximum values, it is observed that a value of 0.802 kN is obtained for the force on the z direction in the case of PA sheets, and of 0.532 kN in the case of PE sheets, respectively, i.e. a ratio of 1.5 in favour of the PA sheets.

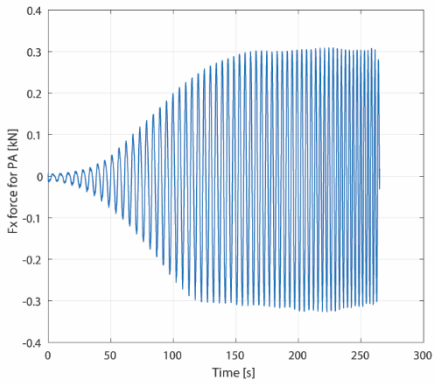

Fig. 15. Force on x-direction for PA sheet

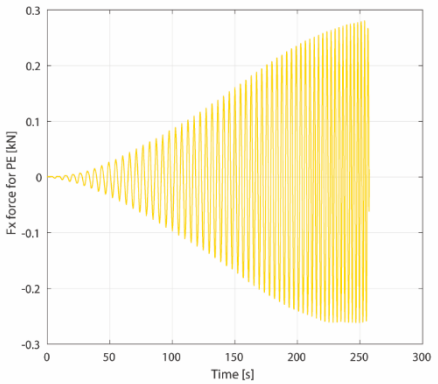

Fig. 16. Force on x-direction for PE sheet

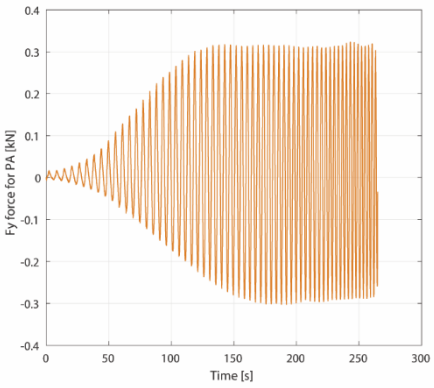

Fig. 17. Force on y-direction for PA sheet

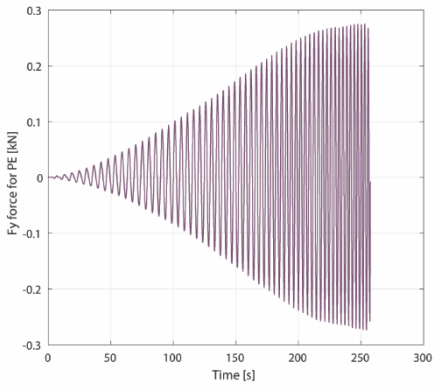

Fig. 18. Force on y-direction for PE sheet

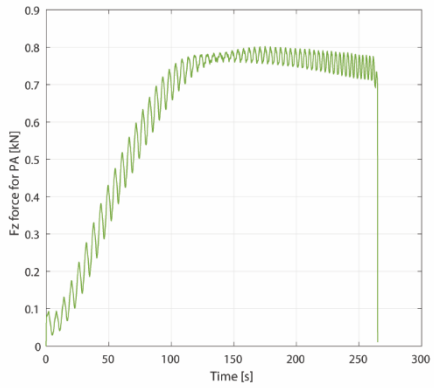

Fig. 19. Force on z-direction for PA sheet

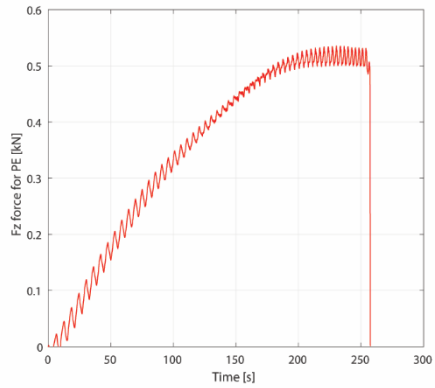

Fig. 20. Force on z-direction for PE sheet

This ratio is correlated with the ratio between the values of the maximum tensile stress for the two types of materials. When considering the forces on the x- and y-directions, their values are much closer: 0.326 ... 0.328 kN for PA sheets and 0.277 ... 0.280 kN for PE sheets. The analysis of the variation graphs shows a remaining at a certain level of the forces on the x- and y-directions, and even a decrease of the force on the z-direction in the case of PA sheets, which is not observed in the case of PE sheets. This is also due to the strong elastic spring back which brings the material back, forcing the punch to process those areas again.

4 Conclusions

The experimental analysis of the behaviour of PA and PE sheets during SPIF leads to the observation that the presence of spring back is much more pronounced than in the case of steel or aluminium alloys, which is normal due to the much lower values of the E modulus. The spring back is significantly more pronounced in the case of PE sheets compared to PA sheets, hence the significant differences between the strains on the x- and y-directions, the major strain and minor strain. The maximum value of the force is influenced by the value of the maximum tensile stress and the value of the Yield stress.

As direction for future research, determining the spring back value for the two types of materials is essential, as knowing the value allows the correction of the punch trajectory so as to obtain parts with the highest dimensional accuracy possible.

References

1. A.K. Behera, R.A. de Sousa, G. Ingarao, V. Oleksik, J. Manuf. Processes, **27**, 37 (2017).
2. P.A.F. Martins, L. Kwiatkowski, V. Franzen, A.E. Tekkaya, M. Kleiner, Cirp Annals-Manufacturing Technology, **58**(1), 229 (2009).
3. M. Durante, A. Formisano, F. Lambiase, Int. J. Adv. Manuf. Technol., **102**(5-8), 2049 (2019).
4. S.A. Yonan, M.B. Silva, P.A.F. Martins, A.E. Tekkaya, eXPRESS Polym. Lett., **8**(5), 301 (2014).
5. F. Maass, S. Gies, A.E. Tekkaya, ESAFORM 2017, *Deformation Characteristics of Thermoplastics in Single Point Incremental Forming*, (Dublin, Ireland, 2017).
6. K.A. Al-Ghamdi, J. Mech. Sci. Technol., **32**(10), 4859 (2018).
7. G. Medina-Sanchez, A. Garcia-Collado, D. Carou, R. Dorado-Vicente, Materials, **11**(9), (2018).
8. I. Bagudanch, Garcia-Romeu, G. Centeno, A. Elias-Zuniga, J. Ciurana, J. Mater. Process. Technol., **219**, 221 (2015).
9. I. Bagudanch, M.L. Garcia-Romeu, M. Sabater, J. Cleaner Prod., **112**, 1013 (2016).
10. A. Formisano, F. Lambiase, M. Durante, J. Manuf. Processes, **58,** 1189 (2020).
11. M.A. Davarpanah, A. Mirkouei, X.Y. Yu, R. Malhotra, S. Pilla, J. Mater. Process. Technol., **222,** 287 (2015).
12. A. Garcia-Collado, G. Medina-Sanchez, M.K. Gupta, R. Dorado-Vicente, Polymers, **12**(8), (2020).
13. N. Cofaru, V. Oleksik, A. Pascu, Proceedings of the 1st WSEAS International Conference on VISUALIZATION, IMAGING and SIMULATION (VIS'08),167 (2008)
14. T. Marques, M. Silva, P. Martins, Int. J. Adv. Manuf. Technol., **60**(1-4), 75 (2012).
15. I. Bagudanch, M.L. Garcia-Romeu, I. Ferrer, J. Ciurana, Rapid Prototyping J., **24**(1), 120 (2018).
16. L.M. Lozano-Sanchez, A.O. Sustaita, M. Soto, S. Biradar, L. Ge, E. Segura-Cardenas, J. Diabb, L.E. Elizalde, E.V. Barrera, A. Elias-Zuniga, J. Mater. Process. Technol., **242,** 218 (2017).
17. A. Mohammadi, H. Vanhove, M. Attisano, G. Ambrogio, J.R. Duflou, ICNFT 2015, *Single point incremental forming of shape memory polymer foam*, (Glasgow, United Kingdom, 2015).
18. M. Hernandez-Avila, L.M. Lozano-Sanchez, I.A. Perales-Martinez, A. Elias-Zuniga, I. Bagudanch, M.L. Garcia-Romeu, L.E. Elizalde, E.V. Barrera, J. Appl. Polym. Sci., **136**(8), (2019).